Curved boundaries and chiral instabilities – two sources of twist in homeotropic nematic tori

James P. McInerney[a], Perry W. Ellis[a,b], D. Zeb Rocklin[a], Alberto Fernandez-Nieves[a,c,d] and Elisabetta A. Matsumoto[*a]

[a] School of Physics, Georgia Institute of Technology, 837 State Street, Atlanta, Georgia, 30332 USA.
[b] John A. Paulson School of Engineering and Applied Sciences, Harvard University, 9 Oxford Street, Cambridge, Massachusetts, 02138 USA.
[c] Department of Condensed Matter Physics, Universitat de Barcelona, Av Diagonal 647, 08028 Barcelona, Spain.
[d] ICREA - Institucío Catalana de Recerca i Estudis Avançats, 08010 Barcelona, Spain.
[†] Electronic Supplementary Information (ESI) available: [details of any supplemen- tary information available should be included here]. See DOI: 10.1039/b000000x/
[*] Corresponding author: sabetta@gatech.edu

1 Microscopic twist instabilities

We seek extremal solutions to the standard Frank-Oseen free energy described in the main text,

$$F = \frac{1}{2} \int_V dV \left[K_1 (\nabla \cdot \mathbf{n})^2 + K_2 (\mathbf{n} \cdot \nabla \times \mathbf{n})^2 + K_3 (\mathbf{n} \times (\nabla \times \mathbf{n})^2 \right]. \tag{1}$$

This is done without shifting the escape away from the centerline. We compute each energy contribution in the coordinates

$$
\begin{aligned}
x &= \left(\rho \cos(\psi) + \xi \right) \cos(\phi), \\
y &= \left(\rho \cos(\psi) + \xi \right) \sin(\phi), \\
z &= \rho \sin(\psi),
\end{aligned}
\tag{2}
$$

writing $dV = \sqrt{g} d\rho d\psi d\phi$ for g the determinant of the metric tensor. We write the director field,

$$\mathbf{n} = \cos(\Lambda)\sin(\Omega)\mathbf{e}_\rho + \sin(\Lambda)\sin(\Omega)\mathbf{e}_\psi + \cos(\Omega)\mathbf{e}_\phi, \tag{3}$$

satisfying the boundary conditions [1]

$$
\begin{aligned}
\Lambda(\rho = 1) = 0, \qquad &\partial_\rho \Lambda(\rho = 0) = 0, \\
\Omega(\rho = 1) = \frac{\pi}{2}, \qquad &\Omega(\rho = 0) = 0.
\end{aligned}
\tag{4}
$$

Since we are particularly interested in the existence of microscopic twisting, we take the ansatz $\Lambda = 0$, $\Omega = \Omega(\rho)$ and search for instabilities to such solutions. Any ψ-dependent Ω or nonzero Λ inherently introduces twisting structure. We integrate over ψ and ϕ obtaining the radial free energy densities f_s, f_t, and f_b for splay, twist, and bend respectively. We then write the Frank-Oseen free energy as $F = K \int d\rho(f_s + \frac{K_2}{K} f_t + f_b) \equiv K \int d\rho f$ and numerically solve the associated Euler-Lagrange equations

$$\frac{\partial}{\partial \Omega} f - \frac{d}{d\rho} \frac{\partial}{\partial \Omega'} f = 0 \tag{5}$$

i

for $\Omega(\rho)$ over the parameter space $\xi \in (1, \infty)$, $\frac{K_2}{K} \in [0, 1]$. These solutions locally extremize Eqn. 1 for the particular $(\xi, \frac{K_2}{K})$ in the $\Lambda = 0$, $\Omega = \Omega(\rho)$ ansatz but are not guarenteed to be stable nor global extrema.

We test the stability of these solutions to perturbations of the form $\delta\Lambda \neq 0$ quantified by the second-order condition [2]

$$\delta^2 F = \sum \frac{\delta^2 F}{\delta u_i \delta u_j} \delta u_i \delta u_j > 0, \tag{6}$$

where $\{u_i = \Lambda, \partial_\rho\Lambda, \partial_\psi\Lambda\}$. To consider this, we write these perturbations as the Fourier series consistent with our boundary conditions

$$\delta\Lambda(\rho, \psi) = \sum_{m,n} c_{mn} \cos\left((\pi/2 + m\pi)\rho\right) \cos(n\psi). \tag{7}$$

We can represent this convergent, infinite sum as the product of finite-dimensional vectors $\mathbf{c} \cdot \delta\mathbf{\Lambda}$. We then rewrite the second-order condition in terms of the matrix elements

$$U_{mnpq} = \delta^2 F[\delta\Lambda_{mp}, \delta\Lambda_{nq}] \tag{8}$$

as $\delta^2 F = \mathbf{c}^T \mathbf{U} \mathbf{c}$ evaluated at $\Lambda = 0$, $\Omega = \Omega^*(\rho)$. Instabilities are then indicated by the existence of negative eigenvalues λ_- of the matrix $\mathbf{U}$ whose eigenvectors $\mathbf{c}_-$ are the coefficients of an energy reducing perturbation since

$$\delta^2 F = \mathbf{c}_-^T \mathbf{U} \mathbf{c}_- = \lambda_- \mathbf{c}_-^T \mathbf{c}_- = -\mid \lambda_- \mid\mid \mathbf{c}_- \mid^2 < 0. \tag{9}$$

While perturbations to Ω may be included in the form $\delta\Omega(\rho, \psi) = \sum d_{mn} \sin(m\pi\rho) \cos(n\psi)$, we find they do not change the observed microscopic twisting instabilities.

2 Dependence of elastic moduli on escape shift σ

Searching for shifts of the escape which minimize the free energy in the main text, we restricted our analysis to the one-constant approximation to explicitly show the shift's dependence on aspect ratio. While the exact values of the elastic moduli certainly affect the σ^* which minimizes the free energy, we find by varying the elastic moduli in two-constant approximations over several orders of magnitude with three different aspect ratios that generically $\sigma^* < 0$ as shown in Fig. 1. Since the preference of shifting is dominated by reductions in splay distortion, $\sigma^* \to 0$ asymptotically as $K_1/K \to 0$. A similar trend is observed as bend distortions become more expensive. Interestingly, the behavior of σ^* at large $K2/K$ appears dependent on aspect ratio.
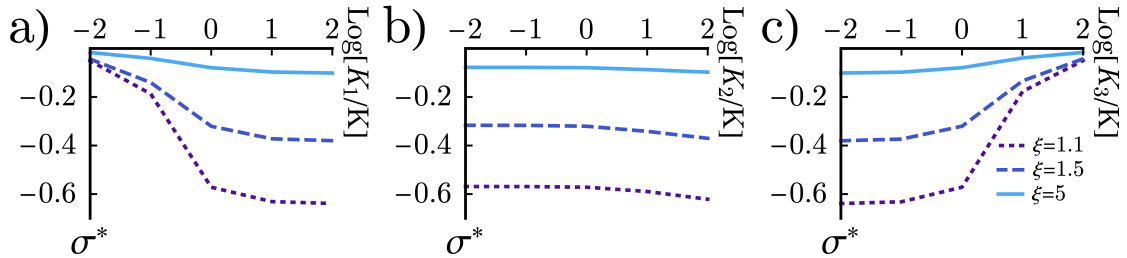

Figure 1: The critical σ^* as a function of change in elastic modulus for a) splay, b) twist and c) bend, show for the aspect ratios $\xi = 1.1, 1.5, 5$.

Fig. 2 shows the effect of the shifted core on the escaped radial profile $\beta(\rho)$ as the aspect ratio of the torus is varied. The β profiles are solutions to the Euler-Lagrange equations using the shifted toroidal coordinates with $\sigma = \sigma^*$ for each value of ξ. When $\sigma = 0$, all $\beta(\rho)$ profiles barely deviate from the cylindrical solution $\Omega(r) = 2\arctan(r)$.
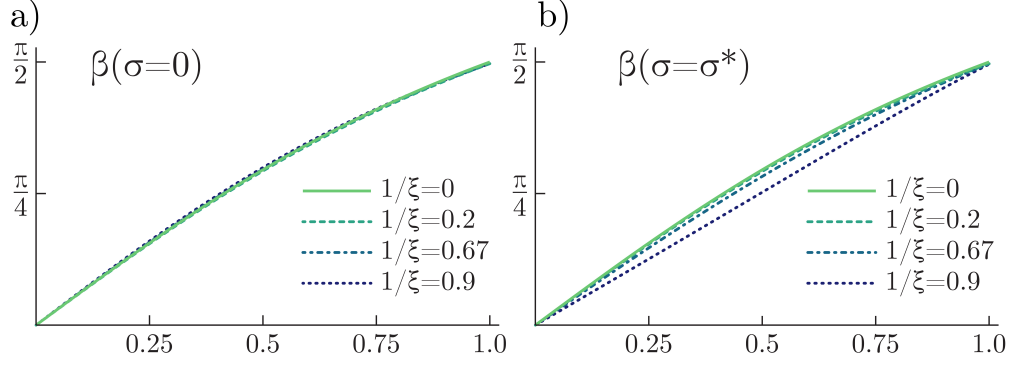
Figure 2: a) The solutions for $\beta(\rho)$ where $\sigma = 0$, for $1/\xi \in \{0, 0.2, 0.67, 0.8\}$. Note that all profiles approximate the cylindrical solution. b) The solutions for $\beta(\rho)$ when $\sigma = \sigma^*$.

3 Energy density

We consider how shifting the escaped core changes the energetics of the twistless homeotropic tori. We solve the Euler-Lagrange equations for the escaped profile $\Lambda(r)$ for the centered torus and $\beta(\rho)$ (evaluated at $\sigma = \sigma^*$) for the shifted core. Fig. 3 shows a 3D rendering of this change in free energy density. The energy is always lowered except for the bend free energy in tori with small aspect ratios (approaching the horn torus limit).
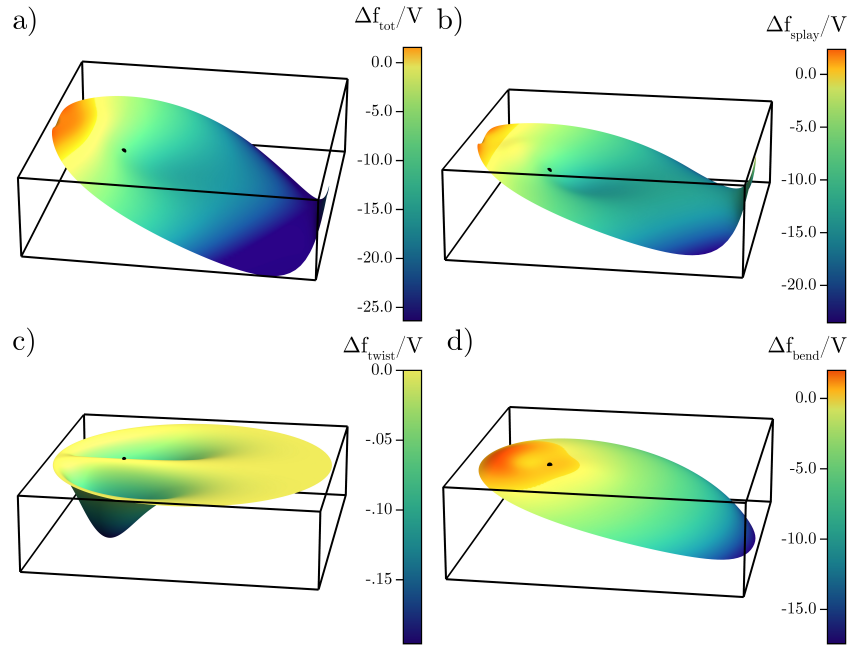

Figure 3: The height maps (a-d) correspond to the density plots in Fig. 4c-f, respectively. They depict the change in free energy density between the centered radial escape $f_i(\Lambda = 0, \Omega(r))$ and the shifted radial excape $f_i(\alpha = 0, \beta|_{\sigma=\sigma^*}(\rho))$, where i denotes one-constant approximation (a), splay (b), twist (c) and bend (d).

References

[1] F. Milan, *MSc thesis*, Leiden University, 2015.

[2] I. M. Gelfand and S. V. Fomin, *Calculus of Variations*, Dover, 2000.